ELSEVIER

Catalysis Today 34 (1997) 411–420

CATALYSIS TODAY

Chapter 11

Kinetics and transport phenomena in heterogeneous gas–solid and gas–liquid–solid systems

Elio Santacesaria

Department of Chemistry, University of Naples, Via Mezzocannone, 4, 80134 Napoli, Italy

1. Introduction to the fundamental laws of transport phenomena

A system can be considered at equilibrium when composition, pressure and temperature are uniform at any point. On the contrary, if differences exist transformations spontaneously occur with mass or energy transfer with a gradual evolution toward equilibrium conditions. Thermal, pressure and concentration gradients are the driving forces for these transformations which can be considered at the different levels: the molecular and macroscopic one.

Molecular transport phenomena are normally much slower than the macroscopic ones; therefore, those phenomena can limit chemical reaction rates. In this paper we will see how and when these limitations occur.

In a fluid, a pressure gradient originates a mass transfer from the high pressure to the low pressure zone. The mass transfer encounters the internal resistance given by the fluid viscosity and the motion can be interpreted with the Newton law:

$$\tau = \pm \mu \frac{\partial u_x}{\partial z} \tag{1}$$

τ being the force of internal friction per unit surface area, μ the viscosity coefficient of the fluid, z a coordinate normal to the direction of the motion x and u_x the speed component in the same direction.

A temperature gradient determines a heat flow from high to low temperature occurring according to the Fourier's law:

$$q = -k \frac{\partial T}{\partial z}$$

= Heat transmitted per unit of time per unit of surface area in the direction z (2)

where k is the thermal conductivity of the fluid and T the absolute temperature.

When concentration gradients are operative and related, for example, to component i, a mass flow of this component from higher to lower concentration occurs according to the Fick's law:

$$J_i = -D_i \frac{\partial C_i}{\partial z}$$

= Number of moles i diffusing in the unit of time per unit of surface area in z direction (3)

It is opportune to remark that the similarity of the three fundamental laws of transport is justified because these laws can be derived from a unique physical model based on the molecular

0920-5861/97/$32.00
PII S0920-5861(96)00063-6

properties. As a matter of fact, transport phenomena are influenced from the motion of the molecules and their interactions. A general equation of the transport can be derived from the kinetic molecular theory of gases:

$$G(y) = n\bar{u}\lambda\frac{\partial y}{\partial z} \tag{4}$$

where λ is the free mean path of the molecules, $\bar{u}$ the mean velocity of the molecules, n the molecular concentration, and y the transport property.

On the basis of the kinetic molecular theory, relations can be given for μ, k and D_i, as function of molecular properties. These relations are valid for very low pressure gases, approaching the properties of ideal gases. Processing these relations, even taking account of the mass of the molecules and their interactions, gives the following expressions:

$$\mu = 2.6693 \times 10^{-5}\frac{\sqrt{MT}}{\sigma^2\Omega_\mu}\left(\frac{\text{g}}{\text{cm s}}\right) \tag{5}$$

$$k = 1.989 \times 10^{-4}\frac{\sqrt{T/M}}{\sigma^2\Omega_\mu}\left(\frac{\text{cal}}{\text{cm s K}}\right) \tag{6}$$

$$D_{12} = \frac{1.858 \times 10^{-3}\sqrt{\dfrac{T^3(M_1+M_2)}{M_1M_2}}}{P\sigma_{12}^2\Omega_D}\left(\frac{\text{cm}^2}{\text{s}}\right) \tag{7}$$

It is easy to demonstrate that $D_{12} = D_{21}$. In these relations M is the molecular weight, σ the kinetic diameter of the molecules, Ω_μ and Ω_D, function of k_BT/ϵ, are named collision integral and are tabulated, k_B the Boltzmann constant, ϵ a molecular interaction parameter. Both σ and ϵ can be evaluated from the intermolecular potential relation of Lennard-Jones:

$$\varphi(r) = 4\epsilon_{ij}\left[\left(\frac{\sigma_{ij}}{r}\right)^{12} - \left(\frac{\sigma_{ij}}{r}\right)^{6}\right]$$

$$\sigma_{ij} = (\sigma_i + \sigma_j)/2 \text{ (arithmetic mean)}$$

$$\epsilon_{ij} = \sqrt{\epsilon_i\epsilon_j} \tag{8}$$

where r is the distance between two molecules.

Parameters ϵ and σ can be determined from the critical properties of the molecules. For example $\epsilon/k_B = 0.75T_C$ and $\sigma = 0.8333V_C^{1/3}$. In the presence of more components than two, the properties of the mixture must be defined through an opportune averaging procedure. In the case of the diffusion coefficient of the i component in the mixture, we will have, for example:

$$D_{im} = \frac{1 - y_i}{\sum_j y_i/D_{ij}} \tag{9}$$

The transport phenomena of major interest occurring in heterogeneous catalysis are those occurring at the fluid–solid interface. The motion of the fluid inside the catalyst bed can be turbulent, but at the interface, a thin film of the fluid exists, the boundary layer, through which mass and heat fluxes occur by diffusion. At the boundary layer, concentration and temperature gradients, are, therefore, located. The molar flow rate will be:

$$N_i = k_c(c_{ib} - c_{is})$$

$$= \text{moles of } i \text{ diffused/times surface area} \tag{10}$$

where c_{ib} is the concentration of i in the fluid bulk, and c_{is} the concentration of i on the solid surface. For gaseous mixtures the following relation is more convenient:

$$N_i = k_g(p_{ib} - p_{is}) \tag{11}$$

where p_{ib} and p_{is} are partial pressures of i in the bulk of the fluid and on the solid surface, respectively.

k_c and k_g are related to the molecular diffusion coefficient D_{12} and to the thickness δ of the boundary layer as in the following relations:

$$k_c = \frac{D_{12}}{\delta}\quad k_g = \frac{D_{12}}{\delta RT} \tag{12}$$

Similarly, the heat flow through the boundary layer can be expressed as:

$$q = h(T_b - T_S) = (\text{heat/time} \times \text{surface area}) \tag{13}$$

where h is the heat transfer coefficient related to the thermal conductivity of the fluid and to the size of the boundary layer.

Average transport coefficients between the bulk stream and particle surface can be correlated in terms of dimensionless groups. For mass transfer, the Sherwood number $Sh = k_c\rho/G$ is an empirical function of the Reynolds number $Re = (Gd_p/\mu)$ and the Schmidt number $Sc = (\mu/D\rho)$. Experimental data are normally correlated in terms of j-factors:

$$j_D = Sh \times Sc^{2/3} = \frac{\alpha}{\epsilon} Re^{-\beta} \quad (14)$$

where G is the mass velocity based upon cross-sectional area of empty reactor, μ viscosity of fluid, ρ density of the fluid, d_p diameter of catalyst particles, D molecular diffusivity of the transferred component, ϵ void fraction of the catalyst bed. α and β must be experimentally determined for a defined system. For a tubular reactor working at $Re > 10$ it results in $\alpha = 0.458$ and $\beta = 0.407$.

A similar approach can be followed also for the estimation of h, the heat transfer coefficient and we will have:

$$j_H = \frac{h}{C_p G} Pr^{2/3} = \frac{\alpha}{\epsilon} Re^{-\beta} \quad (15)$$

in accordance with the analogy proposed by Chilton and Colburn. Pr is the Prandtl number $Pr = \mu C_p/k$, with C_p = specific heat and k = thermal conductivity of the fluid. Therefore, a correlation exists between J_H and J_D according to which it is possible to write $J_H \simeq 1.08 J_D$.

2. Temperature and concentration gradients set from the chemical reaction

When a solid porous catalyst is employed to promote a chemical reaction, this occurs mainly inside catalyst particles consuming reagents, giving products, and absorbing or releasing heat. The chemical reaction is, therefore, responsible for both the temperature and concentration gradients. These gradients are first originated inside the pores of the catalyst particles, diffusion occurs here together with the chemical reaction. For higher reaction rates we have significant gradients also in the boundary layer at the external fluid–solid external interface. The following possibilities can be distinguished:

(1) Reaction rates depend on the extension of the catalytic surface area. In this case, gradients are negligible and we can measure the true chemical reaction rate.

(2) Reaction rates are limited from the resistance to the internal diffusion of reagents or products. In this case, we have a concentration profile of each component, inside the particle different from the concentration on the external catalytic surface.

(3) When the reaction is exothermic or endothermic we can have also a temperature profile inside the catalyst particles.

(4) A temperature gradient can be operative at the boundary layer. As a consequence the temperature of the fluid flowing can be different from that of the external catalytic surface.

(5) Reaction rates are limited by the resistance to the external diffusion at the boundary layer.

All the situations mentioned can be seen as particular kinetic regimes and treated separately. In the gas–liquid–solid reactors, gradients 3 and 4 can be neglected for the high thermal conductivity of the liquid wetting the solid. By increasing reaction rates, the regimes involved pass from 1 to 5.

3. Kinetic regime and reaction rates. Determination of mass transfer parameters

Let us consider now in detail the five possible kinetic regimes mentioned before.

3.1. Regime 1. Intrinsic chemical reaction kinetics

This case is characterized by negligible gradients and is an ideal situation for the laboratory kinetic runs. The measured reaction rates are, in this case, true chemical reaction rates not limited or affected from diffusional resistances.

3.2. Regime 2. Reaction rate influenced by internal diffusion

The diffusion of reagents and products inside the pores of the catalyst occurs together with the reaction, that is, the two processes are simultaneous and not consecutive. For this reason, the influence of the internal diffusion in limiting the reaction rate must be described introducing this limitation in the reaction rate relationship. For a reaction of order n we will have, for example:

$$r = \eta k_n C_{A_s}^n \tag{16}$$

where η is the effectiveness factor:

$$\eta = \frac{\text{observed reaction rate}}{\text{intrinsic chemical reaction rate}} \tag{17}$$

that is, η is a factor describing the effect of the internal diffusion on the reaction rate. In the same relation, C_{A_s} is the concentration of the reagent A on the catalyst surface.

The effectiveness factor is related to the Thiele or Weisz modulus, the first being useful when the goal is the reactor modeling and the kinetic equation is known, the second being used when data of the reaction rate are available but the kinetic equation is still unknown. The mentioned moduli are respectively:

$$\text{Thiele modulus } \phi = \sqrt{\frac{kC_{A_s}^{n-1}}{D_{\text{eff}}}} \tag{18}$$

$$\text{Weisz modulus } M_w = \phi^2\eta = \frac{r_A L^2}{C_{A_s} D_{\text{eff}}} \tag{19}$$

where L is the volume of the catalyst particles/external surface, that is, L is a shape factor equal to $R/2$ for cylinders, $R/3$ for spheres, thickness/2 for slabs etc. The relations of η with ϕ change with the shape of the catalyst particles: we will have for example:

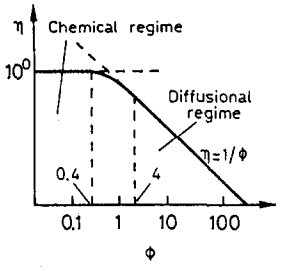

Fig. 1. Plot of the effectiveness factor as a function of the Thiele modulus.

$$\text{Slabs } \frac{1}{\phi} tgh\phi \tag{20}$$

$$\text{Spheres } \frac{1}{\phi}\left(\frac{1}{tgh3\phi} - \frac{1}{3\phi}\right) \tag{21}$$

Fig. 1 and Fig. 2 report the plots of η versus ϕ and M_w, respectively, for the spherical particles of the catalyst calculated for a first order reaction. It is useful to observe that for the first order reactions, the Thiele modulus ϕ is independent of the surface concentration of the reagent.

Observing the plots reported in Fig. 1 and Fig. 2, two large asymptotic zones can be recognized: the first characterized by the chemical regime ($\phi < 0.4$ or $M_w < 0.15$) and the second in which internal diffusion limitations are predominant ($\phi > 4$ and $M_w > 7$). In this last case

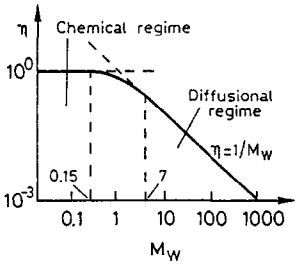

Fig. 2. Plot of the effectiveness factor as a function of the Weisz modulus.

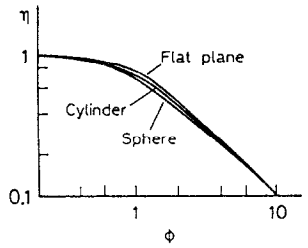

Fig. 3. Effect of the shape of the catalyst particles on the effectiveness factor in relation to the Thiele modulus.

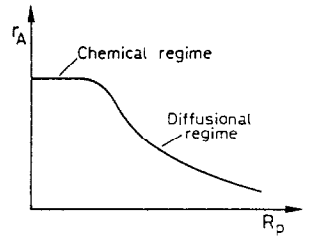

Fig. 5. Evolution of the reaction rate with the particle radius.

the effectiveness factor can be calculated in a simplified way as $\eta = 1/\phi = 1/M_w$.

In the intermediate zone a more rigorous calculation of η is necessary, but if the asymptotic approximation is adopted also in this case the error introduced in the calculation of η is less than 5%.

The effect of the shape of the catalyst particles on the effectiveness factor is moderate as can be seen in Fig. 3. The effect of the reaction order is small, too, as it can be observed in Fig. 4.

The influence of the internal diffusion on the reaction rates can be shown by two types of experiences: (i) the determination of the reaction rates in the presence of catalyst particles of different sizes, (ii) the determination of the reaction rates for a given size at different temperatures. In the first case, as the effectiveness factor is very sensitive to the particle sizes, the reaction rate strongly decreases by increasing the catalyst particle size as shown in Fig. 5. In this case, the effectiveness factor η can be determined directly as the ratio of the reaction rates in the diffusional and chemical regime, respectively. As to the second case if we plot the logarithm of the reaction rate as a function of the temperature reciprocal, when the internal diffusion is operative, a trend as that reported in Fig. 6 is obtained.

The apparent activation energy corresponding to the diffusional regime will be about 1/2 of that in the chemical regime, that is the mean between the activation energy of the chemical reaction observed at lower temperature and that of the diffusional process which is very low.

To evaluate the effectiveness factor η, it is necessary to determine D_{eff}, effective diffusional coefficient, using the following relations:

$$\frac{1}{D_{eff}} = \frac{1}{D_{be}} + \frac{1}{D_{ke}} \tag{22}$$

where D_{be} = bulk diffusion coefficient, that is, the diffusion coefficient of the fluid in the macropores, D_{ke} = Knudsen diffusion coefficient, that is, diffusion in micropores.

$$D_{be} = \frac{D_{12}\theta}{\tau} \tag{23}$$

$$D_{ke} = 1.94 \times 10^4 \frac{\theta^2}{\tau S_g \rho_p} \sqrt{\frac{T}{M}} \tag{24}$$

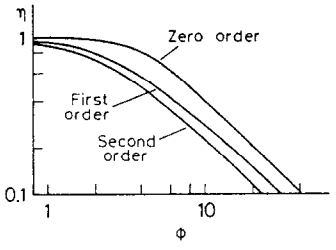

Fig. 4. Effect of the reaction order on the effectiveness factor in relation to the Thiele modulus.

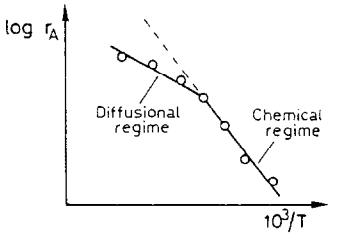

Fig. 6. Effect of internal diffusion on the apparent activation energy.

θ being the porosity of the solid, τ the tortuosity factor, a factor depending on the porosity characteristics of the catalyst which values can be assumed in the range 0.3–10, S_g the specific surface area of the catalyst, and ρ_p the catalyst particle density.

The rigorous evaluation of the effectiveness factor η requires the definition of the profile of the reagents concentrations inside the catalyst particles. For spherical particles, in steady state conditions, the profile is obtained by solving the following differential equation derived from the mass balance:

$$\frac{1}{r^2}\frac{d}{dr}\left(r^2\frac{dc}{dr}\right) = \frac{r_A}{D_{eff}} \tag{25}$$

with the following boundary conditions: $c = c_S$ at $r = R$ and $dc/dr = 0$ at $r = 0$.

The solution is normally obtained with iterative numerical procedures. Sometimes, D_{eff} is experimentally evaluated because calculated values can be doubtful especially for the value to be attributed to the tortuosity factor τ.

3.3. Regime 3. Effects of the intraparticle temperature gradient

The temperature gradient inside the catalyst particles reflects the corresponding concentration gradient and depends on the reaction enthalpy. Indeed, the heat balance on a single particle gives place to a relation quite similar to that obtained from mass balance [see relation (25)]:

$$\frac{1}{r^2}\frac{d}{dr}\left(r^2\frac{dT}{dr}\right) = \frac{(-\Delta H)r_A}{k_{eff}} \tag{26}$$

with the boundary conditions $r = R$ when $T = T_S$ and $dT/dr = 0$ for $r = 0$. k_{eff} is the thermal conductivity of the solid, ΔH the reaction enthalpy.

Eliminating the common terms between relations (25) and (26), we obtain:

$$T - T_S = \frac{D_{eff}}{k_{eff}}(C_s - C)(-\Delta H) \tag{27}$$

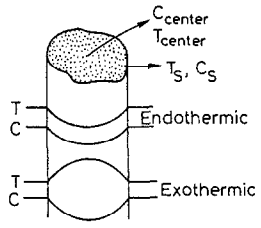

Fig. 7. Temperature and concentration gradients in a catalyst particle for, respectively, an endothermic and an exothermic reaction.

that is, for any value of C inside the particle, we have a corresponding value of T. Therefore, it is sufficient to evaluate the concentration profile because with relation (27) the temperature profile is promptly defined. An example of the profiles obtainable is reported in Fig. 7.

When $C_{center} \simeq 0$, we have $\Delta C \simeq C_s$; in this case, we have ΔT_{max}, that is:

$$\Delta T_{max} = \frac{D_{eff}}{k_{eff}} C_s(-\Delta H) \tag{28}$$

This value gives an idea of the importance of the temperature gradients in affecting reaction rates ΔT_{max} can be referred to the surface temperature T_s, that is, $\beta = \Delta T_{max}/T_s$ is called the 'Prater number'.

Catalysts are normally insulating materials; nevertheless, their thermal conductivities are much higher than those of the reacting gases. For this reason, in steady state conditions, the internal temperature gradient is seldom important in practice. When this gradient is present, the effectiveness factor can assume values greater than one as shown in Fig. 8 and Fig. 9 where plots for $\eta - \phi$ and $\eta - M_w$ are reported for different of values E/RT_s and of the Prater number.

The internal temperature gradient can produce thermal shock to the catalyst particles followed by breaking and sintering. The temperature inside the particle can be measured inserting a thin thermocouple.

3.4. Regimes 4 and 5. External gradients

Also in these cases, the chemical reaction consuming the reagents is responsible for the

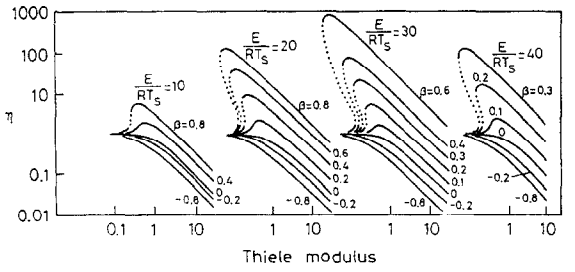

Fig. 8. Plots of the effectiveness factor against the Thiele modulus in the case of both exothermic and endothermic reactions with an internal temperature gradient.

gradients. These will fall between the two limits:

$$\Delta C_{min} = C_b - C_s \cong 0 \text{ that is } C_b \cong C_s$$

$$\Delta C_{max} = C_b - C_s \cong C_b \text{ that is } C_s \cong 0 \qquad (29)$$

where C_b is the bulk concentration of the reagent and C_s the concentration on the external surface of the catalyst. If the reaction is exothermic or endothermic together with the concentration gradient we also have a temperature gradient at the interphase.

In Fig. 10 and Fig. 11 examples of gradients are reported which could be obtained at the catalyst interphase for an exothermic and an endothermic reaction, respectively.

To evaluate the influence of the external transport phenomena on the reaction rate, the fluid dynamic conditions of the reactor must be known. In this case, diffusion and reaction are consecutive steps and can, therefore, be treated separately. Moreover, when necessary, we can apply the useful approximations of the slow step

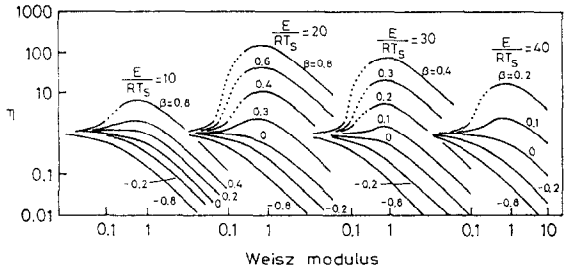

Fig. 9. Plots of the effectiveness factor against the Weisz modulus in the case of both exothermic and endothermic reactions with an internal temperature gradient.

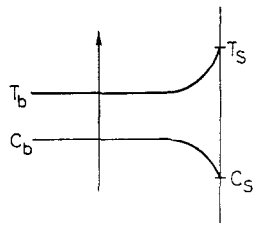

Fig. 10. Typical external gradients of temperature and concentration in the case of an exothermic reaction.

or of the steady state. Applying this latter we have, for example:

$$r = k_m a_m (C_b - C_s^n) = kC_s \qquad (30)$$

where a_m is the external surface area of the catalyst. C_s can be determined and introduced in either of the two members. In the case of $n = 1$, we obtain, for example:

$$C_s = \frac{C_b}{1 + \dfrac{k}{k_m a_m}} \Rightarrow r = \frac{c_b}{1/k + 1/k_m a_m} \qquad (31)$$

To the contrary, by assuming the slow step approximation, the two limit conditions initially described are obtained, that is:

$$\Delta C \simeq 0 \quad r = kC_b^n \text{ Chemical regime}$$

$$\Delta C \simeq C_b \quad r = k_m a_m C_b \text{ Diffusional regime} \qquad (32)$$

External diffusion has a masking effect on the kinetics, for this reason laboratory operative conditions are chosen in such a way to exclude this influence. This can be done with an experimental approach or by calculation. In the experimental approach kinetic runs are performed for different gas linear velocity conditions (i.e. to maintain the same contact time when doubling

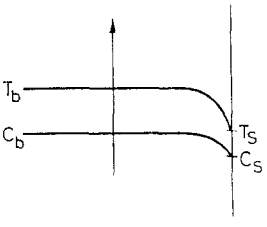

Fig. 11. Typical external gradients of temperature and concentration in the case of an endothermic reaction.

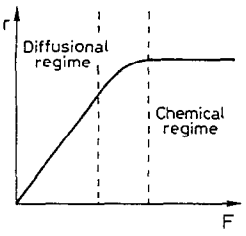

Fig. 12. Effect of the flow rate on the reaction rate in the external diffusional regime.

linear velocity, the catalyst loading should be doubled too). Plots shown in Fig. 12 were drawn. When limitations to external mass transfer are present we could observe an increase in reaction rate on increasing the fluid linear velocity until chemical reaction becomes slower than mass transfer itself. Also kinetic runs, at different temperatures, give a useful indication of the external diffusion occurrence as it will be seen from Fig. 13. Transport phenomena depend weakly by temperature ($E_{att_{diff}} \rightarrow 0$) so their presence is envisaged by a change of slope when plotting ln r vs. $1/T$.

In the transition zone

$$E_{att_{trans}} \cong \frac{E_{att_{chem}} + E_{att_{diff}}}{2} \cong \frac{E_{att_{chem}}}{2}$$

The transport coefficient can easily be determined by calculation through relations of the type already seen in (14) and (15).

Heat transfer can be expressed by the relation:

$$Q = ha_m(T_b - T_s) = k_m a_m(C_b - C_s)(-\Delta H) \quad (33)$$

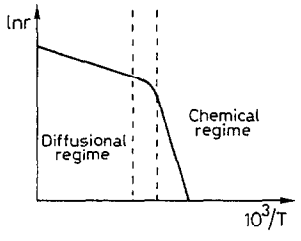

Fig. 13. Effect of the external diffusional regime on the apparent activation energy.

where h is the heat transfer coefficient, T_S the external catalyst surface temperature, T_b the fluid bulk temperature, and ΔH the reaction enthalpy. Therefore, it is again possible to obtain the temperature gradient as a function of the concentration gradient:

$$\Delta T = \Delta C(-\Delta H)\frac{k_m}{h} \quad (34)$$

The heat transfer coefficient can be calculated with empirical relation (15). Putting in (34) k_m and h determined through the empirical relations (14) and (15) we obtain:

$$\Delta T = \Delta C(-\Delta H)\frac{1}{\rho C_p}\underbrace{\left(\frac{C_p \mu/k_f}{\mu/\rho D}\right)^{2/3}}_{\text{Lewis number} \cong 1}\underbrace{\left(\frac{J_D}{J_H}\right)}_{\cong 1} \quad (35)$$

As a consequence:

$$\Delta T \cong \Delta C\frac{(-\Delta H)}{\rho C_p} \quad (36)$$

This relation shows that a significant temperature gradient is possible even though the concentration gradient is very low. Therefore, the concentration gradient can sometimes be neglected, while this is impossible for the temperature gradient. In the case of the reaction:

$$H_2 + \frac{1}{2}O_2 \xrightarrow{(Pt)} H_2O \quad (37)$$

the result was, for example, that for $\Delta C/C_b = 0.05$, $\Delta T = 115°C$. The external temperature gradient is usually more important than the internal one in affecting the reaction rate. In the limit condition for which $C_s \simeq 0$, we will easily calculate the maximum gradient possible:

$$\Delta T_{max} = \frac{C_b(-\Delta H)}{\rho C_p} \quad (38)$$

This calculation can be used as a useful criterion for evaluating the importance of this gradient.

To conclude, in order to evaluate quantitatively the effects of the external mass and the

heat transfer four equations are needed, two corresponding to the physical transport rates and two corresponding to the chemical rates:

$$\left.\begin{aligned} J &= k_m a_m (C_b - C_s) \\ Q &= h a_m (T_b - T_s) \end{aligned}\right\} \text{Physical transport rates} \tag{39}$$

$$\left.\begin{aligned} r &= f(C_s, T_s) \\ Q' &= r(-\Delta H) \end{aligned}\right\} \text{Chemical rates} \tag{40}$$

By introducing the steady state approximation, the needed relations are reduced to two:

$$k_m a_m (C_b - C_s) = f(C_s, T_s) \tag{41}$$

$$h a_m (T_b - T_s) = f(C_s, T_s)(-\Delta H) \tag{42}$$

4. Gas–liquid–solid reactors

For the gas–liquid–solid reactors all the observations reported in the previous sections are valid with the exclusion of the following:

(a) In the gas–liquid–solid reactor, thermal gradients can normally be neglected for the high thermal conductivity of the liquids compared with those of the gases.

(b) The resistance to the diffusion within the catalyst pores is higher than that observed in a gas–solid system because the molecular diffusion in the liquid is much slower.

(c) Transfer phenomena at the gas–liquid interphase could give reaction rate limitations. That is, an additional interphase must be considered.

(d) Kinetic runs are normally performed in batch reactors instead of continuous tubular reactors, as in the gas–solid system.

Let us consider a reaction of the type:

$$\underset{\text{(gas)}}{A} + z\,B \rightarrow P \tag{43}$$

and suppose that the reaction is of first order in respect of the gaseous reagent. By applying the steady state approximation to all the possible steps occurring before and after the reaction and

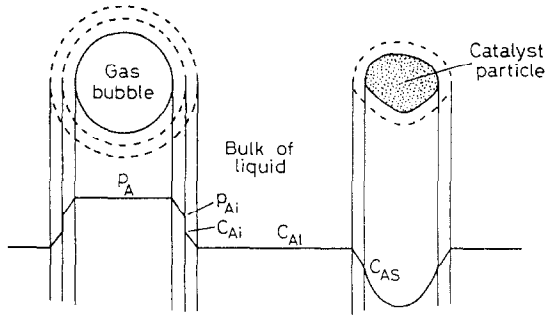

Fig. 14. A picture of the gradients that could be possible in a slurry reactor.

considering all the possible gradients depicted in Fig. 14, we can write.

$$\text{Overall reaction rate} = r_A = \tag{44}$$

$$= k_g a_L (p_A - p_{Ai}) = \text{Gas liquid mass transfer (gas side)}$$

$$= k_L a_L \left(\frac{p_{Ai}}{H} - C_{A_L}\right) \text{Gas liquid mass transfer (liquid side)}$$

$$= k_s a_s (C_{A_L} - C_{A_s}) = \text{Liquid solid mass transfer}$$

$$= \eta k_1 a_s C_{A_s} = \text{Internal diffusion and chemical reaction rate}$$

where a_L is the gas–liquid interphase area, a_s the liquid–solid interphase area, and H the Henry solubility constant for A.

Combining the different relations with the elimination of the interphase concentrations, we obtain:

$$r_A = \frac{p_A}{\frac{1}{k_g a_L} + \frac{H}{k_L a_L} + \frac{H}{k_s a_s} + \frac{H}{\eta k_I a_s}} \tag{45}$$

Normally $1/k_g a_L$ can be ignored, mainly when a pure gas reagent is used. As $a_s = 6m/\rho_p d_p$, where m is the catalyst hold up, ρ_p the density of catalyst particle and d_p the particle diameter, we can obtain by substituting in relation (45):

$$\frac{p_A}{H r_A} = \frac{1}{k_L a_L} + \frac{\rho_p d_p}{6m}\left(\frac{1}{k_S} + \frac{1}{\eta k_1}\right) \tag{46}$$

that is, a linear correlation exists between p_A/Hr_A and $1/m$. When the reaction order is different from 1 this linear correlation is not valid. The description of reactions with orders different from one requires the determination of the concentration profiles of the gaseous reagent inside the catalyst particles. The parameters of the kinetic model, useful for describing gas–liquid–solid reactors are k_L, a_L, k_s, a_s, H, k_n and η. Many of them would be determined independently with respect to the chemical reaction in order to avoid statistical correlation.

5. For further reading

J.M. Smith, Chemical Engineering Kinetics, McGraw Hill, 1981.
S. Carrà and L. Forni, Aspetti Cinetici della Teoria del Reattore Chimico, Tamburini Editore, 1974.
S. Carrà, V. Ragaini and L. Zanderighi, Operazioni di Trasferimento di Massa, C. Manfredi Editore, 1969.
L. Forni, Fenomeni di Trasporto, Edizioni Cortina, 1979.
C.N. Satterfield and T.K. Sherwood, The Role of Diffusion in Catalysis, Addison-Wesley, 1963.
R.E. Treybal, Mass Transfer Operation, McGraw Hill, 1968.
R.B. Bird, W.E. Stewart and E.N. Lightfoot, Fenomeni di Trasporto, Casa Editrice Ambrosiana, 1970.
O. Levenspiel, The Chemical Reactor Omnibook, OSU Book Stores, Oregon, 1984.
J.A. Wesseling and R. Krishna, Mass Transfer, Ellis Horwood, 1990.
J.J. Carberry, Physico-Chemical Aspects of Mass and Heat Transfer in Heterogeneous Catalysis, in Catalysis, Vol. 8, 1987, p. 131.
P.A. Ramachandran and R.W. Chaudari, Three-Phase Catalytic Reactor, Gordon and Breach, 1983.
C.N. Satterfield, Heterogeneous Catalysis in Practice, Addison-Wesley.
M. Dente and E. Ranzi, Principi di Ingegneria Chimica, CLUP, 1977.
G. Biardi, Reattoristica Chimica, CLUP, 1976.
S. Carrà, Chim. Ind., 54(5) (1972) 148.
C.H. Bamford, C.F.H. Tipper and R.G. Compton, Comprehensive Chemical Kinetics, Vol. 23, Elsevier, Amsterdam, 1984.